# Electrochemical and Photoelectrochemical Behavior and Selective Etching of III-V Semiconductors in H<sub>2</sub>O<sub>2</sub> as Redox System

## Edouard Haroutiounian and Jean-Paul Sandino

R.T.C. La Radiotechnique-Compelec, Laboratoire de Chimie, 92156 Suresnes, Cedex, France

## Paul Cléchet,\* Didier Lamouche, and Jean-René Martin

Laboratoire de Physicochimie des Interfaces, Ecole Centrale de Lyon, B.P. 163, 69130 Ecully, France

#### ABSTRACT

Basic electrochemical processes at GaAs, GaAsP, and GaAlAs electrodes were studied in  $H_2O_2$  aqueous solutions at several pH values. An analytical automatic system, which directly plots gallium concentration vs. potential, allows the collection of information on corrosion processes. The approach of making continuous analysis of gallium ions, while dissolving the semiconductor at a preselected potential, was used in conjunction with impedance and ellipsometric measurements in order to study interfacial phenomena. On the basis of these results, a mechanism for chemical corrosion (etching) which involves electrons captured from semiconductor surface states by  $H_2O_2$  was proposed. Anodic polarization can also induce corrosion by hole generation in the valence band or by avalanche breakdown. As expected, pH plays a fundamental role in the corrosion process through the solubility shift of the oxide layer. Further consideration is given to the effect of illumination, with special emphasis on p-type semiconductors, for which it can lead to an inhibition effect on corrosion via a current doubling mechanism. Finally, application of selective etching is described for GaAs, GaAlAs, and GaAsP hetero structures.

Selective etching has been the subject of a number of investigations of interest in connection with III-V semiconductor devices, heterojunction laser technology, and more general multilayer device technology (1, 2). For practical purposes, the dissolution is generally carried out by using redox etchants, without a thorough knowledge of the mechanisms leading to the selective corrosion phenomenon (3-6). The result is a semiempirical approach which is time consuming when a new specific problem is encountered.

Solar energy conversion has stimulated fundamental research in the field of semiconductor electrochemistry (7-9), and processes associated with semiconductor interfaces are now better understood. However, this knowledge is still very difficult to exploit directly for the investigation of redox systems that might be suitable for selective etching. From a practical point of view, it means that the corrosion behavior of a particular semiconductor has still to be explored in detail experimentally. To solve such problems, the choice of the perfect tool is not obvious. Since corrosion involves electron exchange through a solid-liquid interface, it follows that electrochemical tools seem to be the most appropriate. In the first instance, current-voltage curves are generally obtained. However, it has been observed in oxidizing media, and this point will be discussed at length later in this paper, that the anodic corrosion current of a n-type semiconductor in the dark is sometimes exactly compensated for by electrons captured by the etchant over a large potential range (2, 10-13). No information can be obtained about the corrosion rate for such situation from classical voltamperometry. This necessitates an alternative way of gaining further insight into the electrochemical behavior of semiconductors.

The rotating ring-disk electrode (RRDE), which has been largely used for semiconductor corrosion studies (see, for example. Ref. 14-17), does not perfectly suit our gas evolving etchant  $(H_2O_2)$ . Direct sequential chemical analysis of corrosion products may give valuable information, especially since the gallium ion concentration vs. time can be converted into current voltage curves. Such a method would be tedious and time consuming unless a fast automatic system for

Electrochemical Society Active Member.
 Key words: etching, semiconductor, H<sub>2</sub>O<sub>2</sub>, photoelectrochemistry, corrosion mechanism, passivation, semiconductor technology, GaAs/GaAsP/GaAlAs.

Ga analysis were available. Consequently, we have developed a method of investigation based on the use of an automatic colorimetric system. Gallium analysis is performed at the outlet of a three-electrode microelectrochemical cell.

As shown later, this method, which can be adapted to redox couples other than the H<sub>2</sub>O<sub>2</sub> used here, can lead to better knowledge of the dissolution process and thus can make the choice of selective etching criteria easier. In the future, this technique might be considered as a complementary tool for electrochemical studies involving, i.e., RRDE. In this study, impedance-electrode measurements and ellipsometry were also used in order to complete the information gained from the gallium concentration curves.

### Experimental

Materials.—Unless otherwise specified, the III-V samples used in this study were (100) single crystals. n-Type gallium arsenide was Si-doped bulk material with donor density  $N_{\rm D}\sim 10^{18}~{\rm cm}^{-3}$ , n-type Ga<sub>0.7</sub>Al<sub>0.3</sub>As (Si doped.  $N_{\rm D}\sim 2\cdot 10^{17}~{\rm cm}^{-3}$ ), and GaAs<sub>0.6</sub>P<sub>0.4</sub> (Te doped.  $N_{\rm D}\sim 4\cdot 10^{16}~{\rm cm}^{-3}$ ) were vapor phase epitaxial layers grown on (100) GaAs substrate, with a typical thickness of 20  $\mu$ m. Experiments on GaAs were performed after etching in H<sub>2</sub>SO<sub>4</sub>/H<sub>2</sub>O/H<sub>2</sub>O<sub>2</sub> (3:1:1) in order to remove the superficial damaged layer. The ohmic contacts were made using alloyed tin on the back of the GaAs substrate under N<sub>2</sub> or H<sub>2</sub>/N<sub>2</sub> controlled atmosphere.

Apparatus.—The microelectrochemical cell with continuous electrolyte flow (4 ml mn<sup>-1</sup>) is shown Fig. 1. Its general design was drawn from Ref. (18) with some modifications. The electrode (0.2 cm<sup>2</sup>) can be illuminated, via an optical fiber, with a 100W halogen lamp. In order to prevent thermal effects due to IR radiation, a filter (wavelength bandpass: 400-650 nm) and an absorption cell filled with water (2 cm thickness) were used.

Experiments were performed using a conventional potentiostatic system (Tacussel Solea S.A.). Successive preselected potentials were applied to the semiconductor electrode for 10 min while the electrolyte flow leaving the cell was analyzed For each voltage, the static current was measured in order to get the corresponding current-voltage curves which, for simplicity, have been drawn as continuous lines in

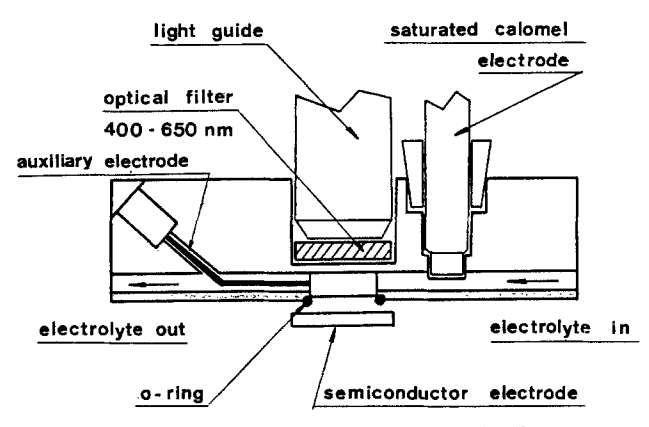


Fig. 1. Plan of the microelectrochemical cell

the various figures. Between two consecutive steps, etching of the semiconductor surface was carried out with the help of the etchant solution described in the previous section and a bypass system. All potentials are expressed with respect to the saturated calomel electrode (SCE).

Electrolyte.-The choice of the electrolytes and redox system was dictated by experience, since citric acid and H2O2 are frequently used for GaAs etching as complexing electrolyte and oxidizing agent, respectively. Moreover, this mixed solution has good selectivity properties for GaAsP/GaAs heterostructures, since only the latter product dissolves. Given the poor buffer capability of citric acid, we also used a phosphate buffer in medium pH range. Experiments in highly acidic and alkaline media were also carried out by adding H<sub>3</sub>PO<sub>4</sub> or NaOH to the solutions. In every case, and unless otherwise specified, a 0.1M concentration for electrolyte and 1% (33.3 ml of 30%) H<sub>2</sub>O<sub>2</sub> per liter) for H<sub>2</sub>O<sub>2</sub> was chosen for experimental convenience. Sodium hydroxide was used for pH adiustments.

Gallium analysis.—At the outlet of the microelectrochemical cell, Ga was analyzed through a colorimetric automatic system (Auto Analyser II, Technicon). The measurement involved the following stages: (i) decomposition of excess  $H_2O_2$  by hydroxylamine treatment; (ii) formation of a colored Ga-rhodamine complex; (iii) extraction of this complex by CCl4; (iv) optical absorption measurements of the organic phase with a spectrophotometer (working wavelength 550 nm).

A calibration curve was drawn with standard solutions of gallium (the stock solution was prepared from high purity Ga metal dissolved in HCl) in the concentration range of interest (0-50  $\mu$ g ml<sup>-1</sup>). Under our experimental conditions, As and Al ions do not interfere in the Ga determination. Relative standard deviation of the calibration curve was 2%. For experiments involving GaAlAs material, a correction factor was used in order to take into account the presence of 30% of aluminum. Conversion of gallium concentrations into current was made by assuming a six-hole corrosion process (19). In order to distinguish clearly the current-voltage curves and the gallium concentration-voltage curves in the text and figure captions, we use I = f(V) for the former and I Ga = f(V) for

Impedance and ellipsometric measurements.—Ellipsometric measurements were carried out with an automatic spectroellipsometer (20). In addition, capacitance measurements were performed with a potentiostatic system, using an ATNE lock-in amplifier and a Hewlett-Packard Model 3325-A function generator, which were controlled by an Apple II microcomputer. The GaAs electrode's area was 0.71 cm2. Unless otherwise specified measurements were made

Table I. Flatband potentials of n-type GaAs, GaAs<sub>0.6</sub>P<sub>0.4</sub>, and  $Ga_{0.7}AI_{0.3}As$ 

рН	n-GaAs	n-GaAso.dPo.4	n-Ga <sub>0.7</sub> Al <sub>0.3</sub> As
0	-1.02*	-1.28 <sup>2</sup> -1.42 <sup>c</sup> -2.0 <sup>a</sup> -2.20 <sup>c</sup>	-1.12a
(H <sub>2</sub> SO <sub>4</sub> , 0.5M)	-1.08b		-1.70d
14	-1.86*		-2.0a
(NaOH, 1M)	-1.88b		-2.4d

Our results.

at a frequency of 1 kHz. Flatband potentials of the freshly etched (called "clean" surface in the text, this term being further justified at the end of the next section) n-type semiconductors, obtained by extrapolation of Mott-Schottky plots calculated from a series equivalent circuit, at two pH's, are shown in Table I. The measured capacitances showed only a weak frequency dependence. The results were perfectly reproducible even after numerous voltage scans. These results are in good agreement with those of other authors (21, 22), except for those of GaAlAs (22). The reason for this discrepancy is not known. The pH dependence of the flatband is about 60 mV per pH unit, except for GaAsP (51 mV per pH unit).

### Results and Discussion

n- and p-Type GaAs.—In order to have a better understanding of the mechanism by which a semiconductor like GaAs corrodes in H<sub>2</sub>O<sub>2</sub> aqueous solution, bearing in mind that such corrosion might be used for selective etching of heterostructures, it is interesting to compare Fig. 2 and 3, which show the results obtained on n- and p-type GaAs in an acidic 1% H2O2 medium, at room temperature.

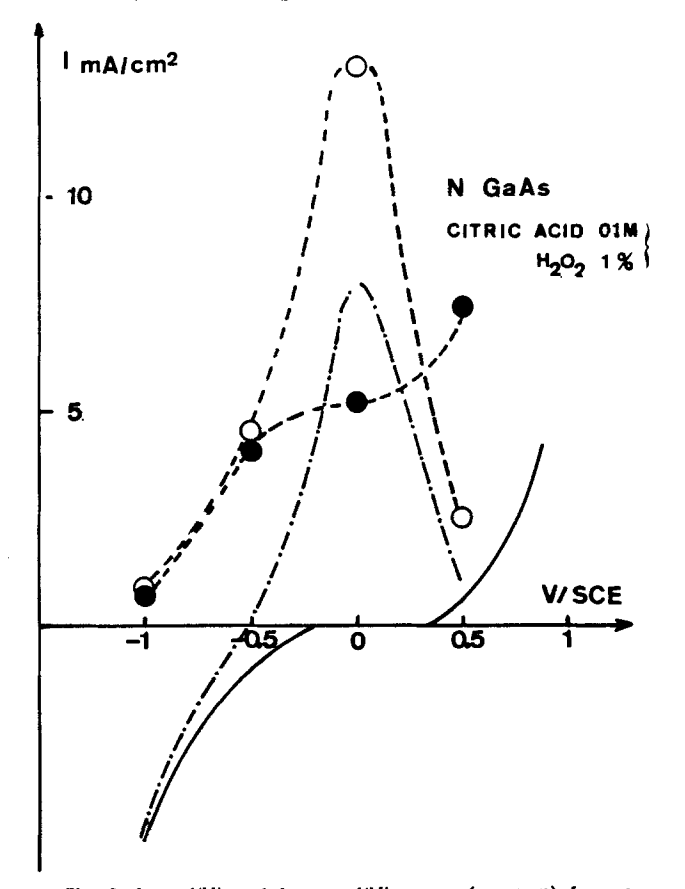


Fig. 2. I = f(V) and  $I_{Ga} = f(V)$  curves (see text) for n-type GaAs in 0.1M citric acid and 1%  $H_2O_2$ .  $--ullet ---I_{Ga}$  in the dark.  $--\bigcirc -I_{Ga}$  under illumination. I = f(V) in the dark. I = f(V) under illumination.

bExtrapolated values from (21). c GaAs<sub>1-x</sub>P<sub>x</sub>: x = 0.39, extrapolated values from (22). d Ga<sub>1-x</sub>Al<sub>x</sub>As: x = 0.27, extrapolated values from (22).

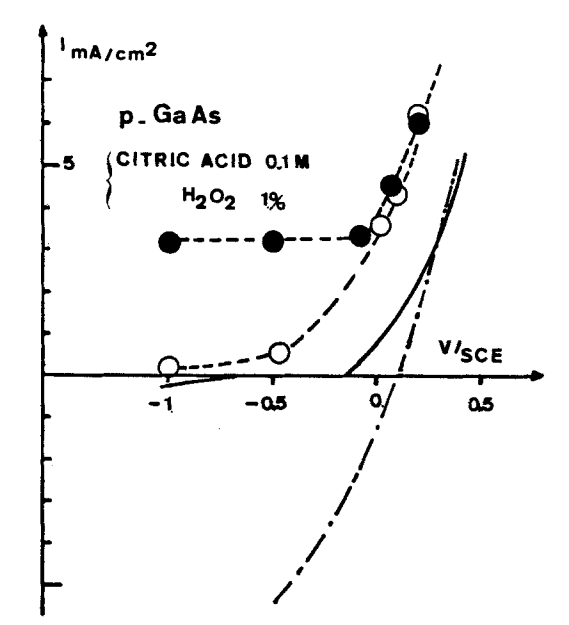


Fig. 3. I=f(V) and  $I_{\rm Ga}=f(V)$  curves for p-type GaAs in 0.1M citric acid and 1%  $\rm H_2O_2$ . Symbols are the same as used in Fig. 2.

With n-type GaAs, in the dark, on anodic scanning, we observe that corrosion begins at about -1.0V. The  $I_{\rm Ga}=f(V)$  curve thus exhibits a characteristic plateau before a sharp increase when the potential reaches +0.5V. As previously stated, the lack of faradaic current in a large range of potential where corrosion occurs (approximately -0.2 to +0.4V) should be noted. Under illumination, the corrosion is accelerated and a maximum appears in the  $I_{\rm Ga}=f(V)$  curve at about the same voltage as the photocurrent peak (see below). This corresponds to a passivation of the semi-conductor.

With p-type GaAs in the dark, the results are comparable. Over a large range of potential (between -1.0 and 0.0V), the corrosion rate remains constant and, as observed with n-type GaAs, this corrosion is not accompanied by a faradaic current.

The behaviors of these two kinds of materials differ strongly under illumination. With p-type, we observe that the corrosion does not increase with illumination, as it does for n-type GaAs; rather it vanishes when a cathodic photocurrent arises.

In order to explain this difference, we must consider the flatband values of these materials at this low pH (-1.15V for n-type and +0.15V for p-type, respectively) and the peculiar redox properties of H2O2 (23, 24). It is well known that  $H_2O_2$  is a strong bifunctional oxidant whose two-step reduction involves an OH radical intermediate. Two "microscopic" standard redox potentials correspond to these two successive steps, the values of which have been estimated by Memming to be widely separated from that of the global  $H_2O_2/OH^-$  system (+1.54V). According to Fig. 4, with p-type GaAs, hydrogen peroxide is capable of giving rise to a current doubling process (23, 24) where each photon induces a two-electron transfer across the interface. The capture of a photoexcited electron from the conduction band creates an OH radical (which has empty levels of low energy) which is then able to inject a hole into the valence band of GaAs. The electric field within the depleted layer being directed towards the bulk semiconductor, the injected holes are driven in this direction. This prevents surface corrosion. This is the reason why no corrosion is observed under illumination with p-type GaAs. This current doubling on p-type GaAs has very recently been observed by Gerischer et al. (25). With n-type GaAs, current doubling is no longer possible, according to the direction of the electric field, which is now

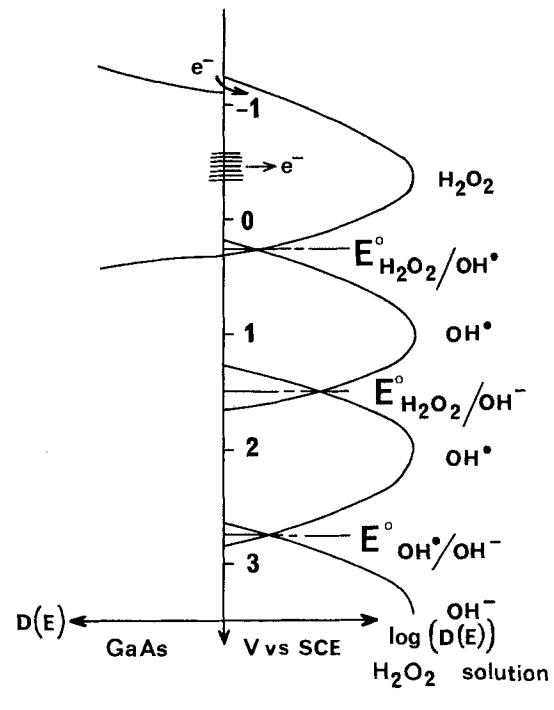


Fig. 4. Energy diagram at pH 2 of the GaAs- $H_2O_2$  interface (24). This diagram supposes an equal concentration of all the redox species. The stationary concentration of OH being small (24), the overlap of the conduction band and of  $H_2O_2$  is probably much better than represented here.

directed towards the surface for this range of potential. Electrons are driven to the bulk, and holes to the surface, where they contribute to semiconductor dissolution while an anodic photocurrent appears (Fig. 2). This situation (increase of  $I_{\rm Ga}$ ) appears as soon as the electrode potential becomes positive of the flatband potential of the material.

The shapes of the curves of Fig. 2 and 3 are easy to interpret at high anodic and cathodic polarization.

With n-type GaAs in the dark (Fig. 2), the sharp increase of the corrosion at strong anodic polarization follows exactly the increase of the anodic current. It has been shown that this wave is an avalanche breakdown wave which depends on doping level and crystallographic defects of GaAs (26). The discrepancy observed between the breakdown voltage shown in Fig. 2 and 5, at the same pH, probably results from the

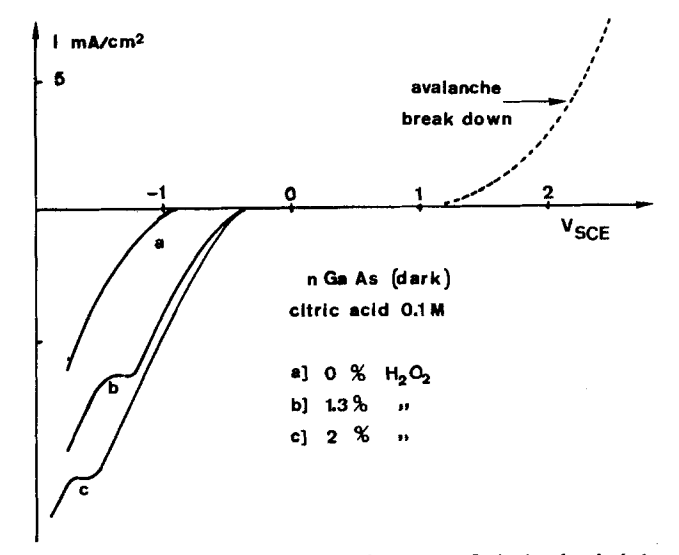


Fig. 5. Voltamperometric curves for n-type GaAs in the dark in 0.1 citric acid and several  $H_2O_2$  concentrations. Voltage scanning rate: 100 mV min $^{-1}$ .

batch origin of the GaAs substrate. For lower potentials, in the dark, the anodic breakdown current disappears while corrosion, as for p-type samples, decreases. The difference lies in the fact that for more negative potentials (less than -0.3V), a large cathodic wave arises and at the same time corrosion stops. It is logical to postulate that this corrosion suppression at low potential is a consequence of the electrolytic reduction of H<sub>2</sub>O<sub>2</sub> at the interface by electrons from the conduction band, which accumulate when the electrode potential approaches its flatband value. This reduction of H2O2 at n-type GaAs electrode under cathodic polarization is indicated by the mass-diffusion limited waves of Fig. 5. The same explanation is given by Gerischer et al. for the observed chemical stability of n-type GaAs in Br2 solution under cathodic polarization (12).

With p-type GaAs in the dark (Fig. 3), such a rapid reduction of  $\rm H_2O_2$  does not occur at the surface under cathodic bias, so the corrosion plateau remains flat even at -1.0V. For potentials more positive than -0.2V, the large anodic wave, which is accompanied by a strong corrosion, probably results from the hole accumulation in the valence band and from the resulting breaking of the chemical bonds of the semiconductor. Illumination has no influence here, because of the migration of the holes towards the bulk semiconductor.

The final point concerns how corrosion can occur in the dark, without electron transfer, in the intermediate range of potentials (-0.5 < V < +0.5 for n-type and V < 0V for p-type).

Such corrosion can only be explained by a purely chemical process, i.e., by an exactly compensated exchange of electric charges between the semiconductor, which is oxidized, and the oxidant, which is reduced. This process can be represented by the following schematic reaction

$$GaAs + 3H2O2 + 6H+ \rightarrow Ga+++ + As+++ + 6H2O$$

The nature of the resulting species depends on the pH and complexing power of the electrolyte. This is evidently the process by which chemical etching of the semiconductor proceeds at the rest potential.

The problem is thus to explain how such a reduction of  $\mathrm{H}_2\mathrm{O}_2$ , at intermediate potential, can be initiated by high energy electrons (Fig. 4), since from the classical theory of electron transfer (7, 9, 10), these electrons can only be captured from the conduction band, whose electron concentration, for these two materials in the dark, is poor. In the absence of pinning of the Fermi level, the electron concentration increases as the potential of the semiconductor becomes more cathodic, but this increase is therefore not consistent with the observed voltage independence of chemical corrosion (see Fig. 3). Another explanation must be found.

It is well known that a high concentration of surface and interface states is always present at the surface of GaAs, especially near the middle of the bandgap (27, 28) and if the surface is oxygen covered (29, 30) as after etching by acidic H<sub>2</sub>O<sub>2</sub> mixture (31). According to experiments conducted in vacuo, these electronic states often result from dangling bonds or a different band structure of surface atoms which have a high reactivity for the solvent (32). This is certainly the case for our highly reactive acid etched surfaces. If an electron from such a surface state (examples of which are drawn Fig. 4) is transferred to an adsorbed  $H_2O_2$ molecule, it will lead to a short lived OH radical, which is consequently attached to a surface atom with a weakened bond to the surface. This OH radical is thus in a favorable situation to capture, directly, a second electron from the same atom, without the constraint of equality between donor and acceptor electronic states levels required by the faradaic transfer through the Helmholtz layer. This leads to a still less strongly attached atom and to the progressive corrosion of the electrode.

This mechanism may explain why the chemical corrosion is potential independent and why it occurs in particular at the rest potential, i.e., under the etching conditions, (-0.075V for p-type and -0.245V for n-type in our case).

Under illumination, for p-type material, electrons are available in the conduction band, which, by means of a current doubling mechanism, prevent the corrosion from continuing (Fig. 3). The current doubling phenomenon is thus more rapid than the chemical corrosion process. This is in agreement with the large photocathodic wave seen in Fig. 3. On the contrary, as previously stated, with n-type semiconductors, photoholes which appear in the valence-band contribute to corrosion by chemical bond breaking (Fig. 2).

This analysis shows that, in addition to anodic electrochemical corrosion resulting from hole accumulation in the valence band (p-type) or breakdown (n-type) and the photoelectrochemical corrosion by photoholes (n-type), simple chemical corrosion is another very important means of corrosion which probably does not only occur by hole injection into the valence band. Without any doubt, surface states play a very important role in the etching mechanism, and this fact is emphasized by the polishing or defect-revealing ability of this kind of etch.

Other semiconductors and pH effect.—Figures 6 and 7 show that in the same acidic corrosive medium, the behavior of GaAsP and GaAlAs can be explained using similar arguments. The values of the flatband potentials of these materials, which are slightly more negative than GaAs (Table I), support this argument. We observe that GaAsP (Fig. 6) exhibits a much lower chemical corrosion rate than the two other n-type materials (compare Fig. 2, 6, and 7).

An etchant is generally composed of an oxidant (here  $H_2O_2$ ) and an acidic or basic solubilizing agent of the amphoteric oxide which grows at the surface of the semiconductor (33). Figure 8 shows that the etching rate (i.e., the chemical corrosion at the rest potential) of GaAs in  $H_2O_2/H_3PO_4$  mixtures at various pH's in the dark support this definition. The solubility of GaAs increases strongly in the regions of low and

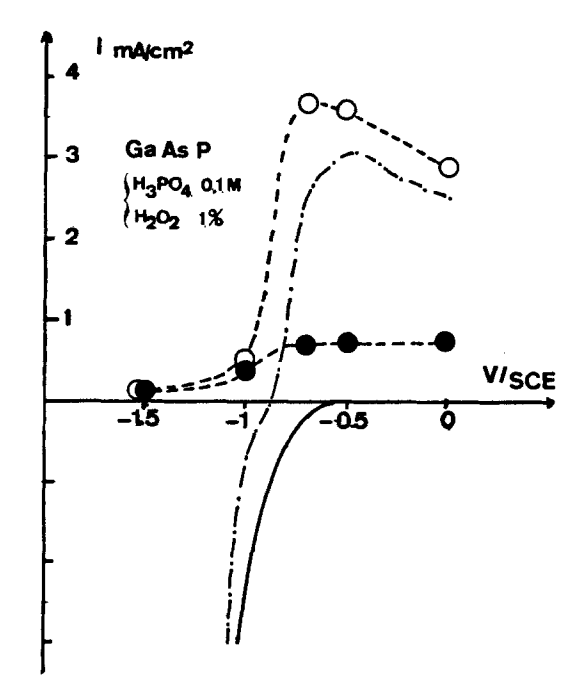


Fig. 6. I=f(V) and  $I_{\rm Ga}=f(V)$  curves for n-type GaAsP in  $H_3PO_4$  0.1M and 1%  $H_2O_2$ . Symbols are the same as used in Fig. 2.

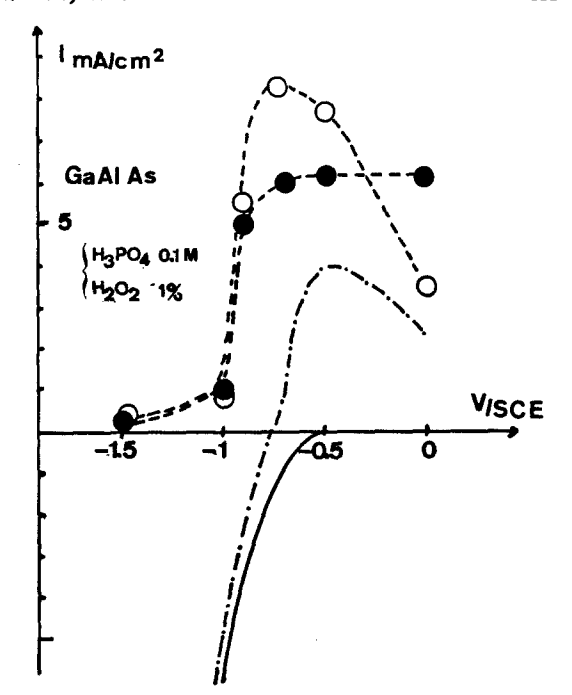


Fig. 7. I=f(V) and  $I_{\rm Ga}=f(V)$  curves for n-type GaAlAs in  $H_3PO_4$  0.1M and 1%  $H_2O_2$ . Symbols are the same as used in Fig. 2.

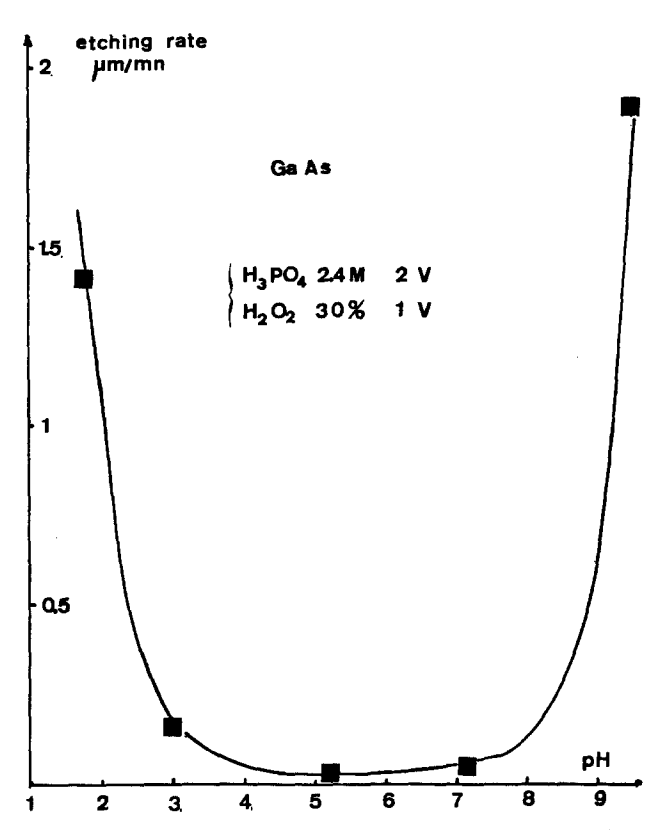


Fig. 8. Etching rate vs. pH curves in the dark of n-type GaAs in 1:2 H<sub>2</sub>O<sub>2</sub> 30% and H<sub>3</sub>PO<sub>4</sub> 2.4M mixture.

high pH when the solubility of the oxides of the different elements of which the semiconductor is composed are known to be large (34). Thus, etching of III-V semiconductors is only efficient at low and high pH and is slow at intermediate values when the low solubility of the oxide protects the material. The two other materials show curves similar to the curve of Fig. 8, except for the lower solubility of GaAsP, which has been already noted. In acidic or alkaline media, this poor etching rate of GaAsP offers selective properties for the removal of GaAs with respect to GaAsP layers in the GaAs/GaAsP heterostructure.

The effect of pH on the etching rate is clearly illustrated by the form of the curves of Fig. 9 obtained at pH 7. The chemical corrosion plateaus practically disappear, while the passivation peaks become very pronounced. Passivation, for these three materials, is very effective for voltages exceeding somewhat the passivation peaks.

On the other hand, at pH 13, Fig. 10-12 show that chemical dissolution is effective again and that the passivation becomes less pronounced.

In the absence of passivation, the corrosion rate is practically proportional to  $H_2O_2$  concentration, as shown Fig. 10 and 12, in the cathodic range of potential (compare the values for  $i_{\rm Ga}$  respectively with 1 and 0.5% of  $H_2O_2$ ). When passivation occurs (as, for example, for GaAlAs and GaAs under illumination at 0.0V), oxide layer formation governs the dissolution process and proportionality with  $H_2O_2$  concentration no longer holds.

All these observations are consistent with a corrosion mechanism which involves competition between the rates of oxide formation and dissolution. The second phenomenon prevails at low and high pH. However, it can also be noted that illumination sometimes reinforces passivation (see Fig. 2, 7, 10, and 12, for instance).

Passivation and oxide layer growth.—Spectroellipsometric and impedance measurements were carried out in order to reveal the effect of oxide growths on the dissolution phenomenon in  $H_2O_2$ . n-Type GaAs was used exclusively for this study.

First, capacitance measurements and Mott-Schottky plots were obtained in citric and phosphoric 0.1M media at pH 2 and 7 without  $\rm H_2O_2$  and for "clean" surface n-GaAs. The data were taken at 1 and 10 kHz. From the Mott-Schottky plots of Fig. 13 we obtained donors densities ( $N_D$ ) of about 7.1  $\times$  10<sup>17</sup> for 10 kHz and 1 kHz, which shows, as previously stated, a very

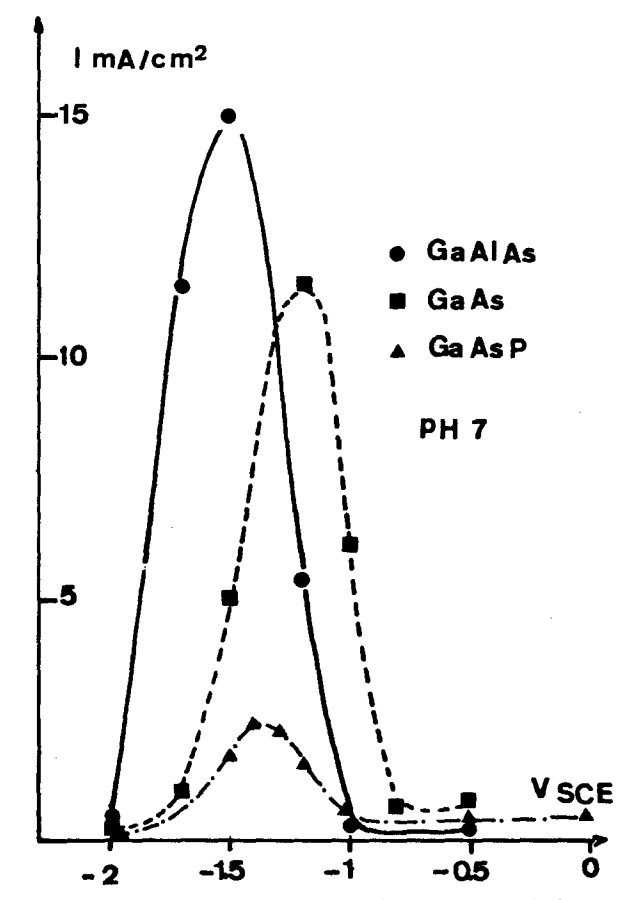


Fig. 9.  $I_{\rm Ga}=\it f(V)$  for n-type GaAs, GaAlAs, and GaAsP in  $\rm H_3PO_4$  0.1M and  $\rm H_2O_2$  1% at pH 7.

weak frequency dependence and a good agreement with the predicted values. No account was taken of

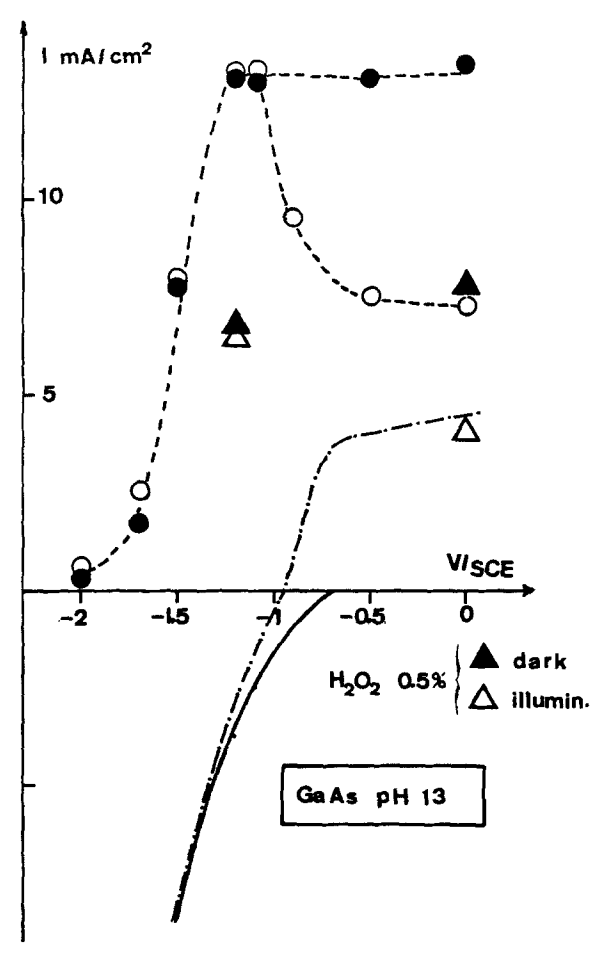


Fig. 10. I=f(V) and  $I_{\rm Ga}=f(V)$  for n-type GaAs in  $\rm H_3PO_4$  0.1M and 1%  $\rm H_2O_2$  at pH 13. Symbols are the same as used in Fig. 2 except for 0.5%  $\rm H_2O_2$  solution.

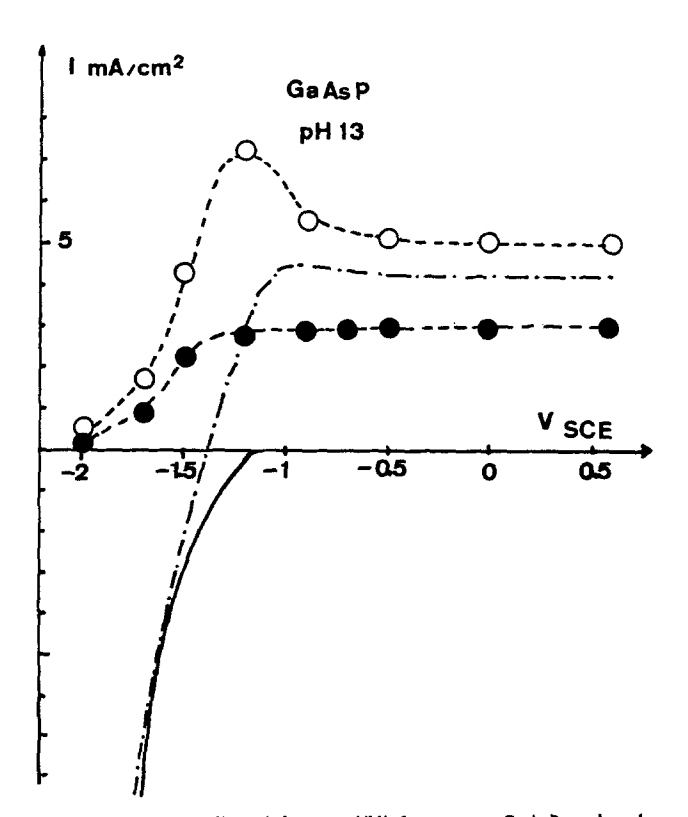


Fig. 11. I = f(V) and  $I_{\rm Ga}$  = f(V) for n-type GaAsP under the same conditions as Fig. 10.

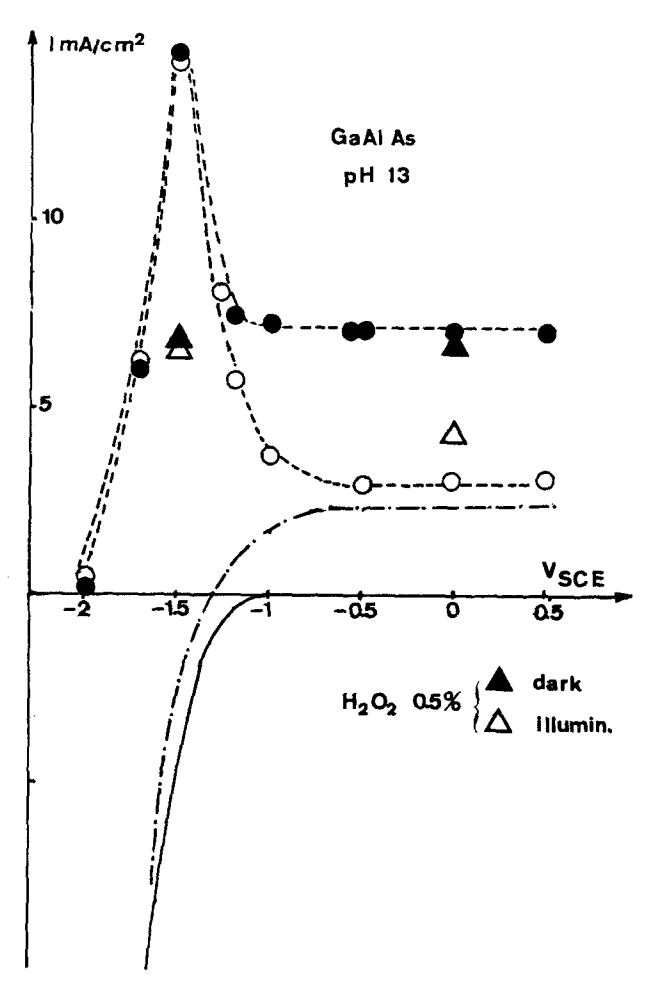


Fig. 12. I=f(V) and  $I_{\rm Ga}=f(V)$  for n-type GaAlAs, in the same conditions as Fig. 10.

surface roughness for the calculation of the doping level. The corresponding flatband potentials were frequency independent and compared favorably, allowing for the observed pH dependence with the values of Table I. Experimental values of these flatband potentials are identical for both solutions (citric and phosphoric), indicating that for a given sample in indifferent electrolyte this quantity is determined by the pH solely. Hence for practical convenience, further experiments were made in a phosphoric medium. The linearities over a large range of potentials of the Mott-Schottky plots (about 1.5V), as well as the perfect reproducibility of these plots even after numerous scans up to the highest voltage attained in capacitance measurements (deep depletion situation), show that the GaAs surface can be considered, from a practical point of view to be oxide free, even if such freshly etched surfaces cannot be considered as completely exempt of oxygen (31). It was impossible to detect the presence of oxide by ellipsometry on surfaces so prepared. This justifies our term "clean."

A second series of capacitance measurements were performed in a  $\rm H_3PO_4$  0.1M +  $\rm H_2O_2$  1% pH 7 medium. These results, which are not shown here, should be discussed in conjunction with the  $\rm I_{Ga}=f(V)$  curve for the n-GaAs of Fig. 9. Several points should be emphasized: (i) the range of potential where Mott-Schottky behavior was observed was very reduced compared to that in the previous media. (ii) The shape of the Mott-Schottky plots seemed to be very time dependent.

These two points clearly support the assumption that in such a medium and for the considered range of potential, changes in the GaAs surface occur in agreement with the observed corrosion and passivation of this material under these conditions.

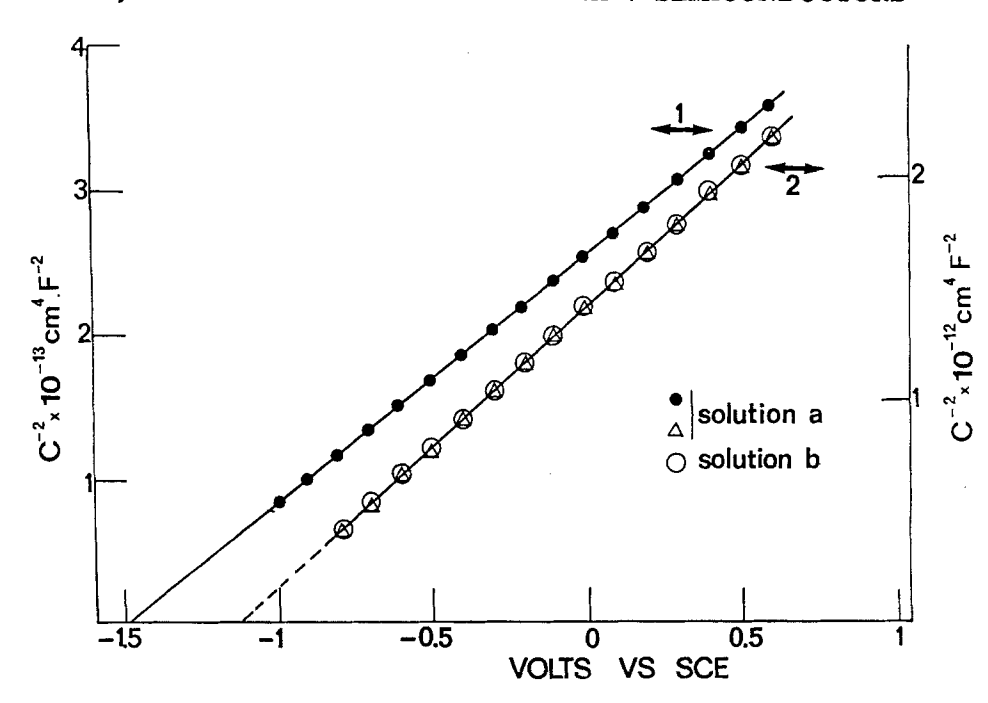


Fig. 13. Mott-Schottky plots for "clean" (1) and oxidized (2) n-type GaAs in: a. H<sub>3</sub>PO<sub>4</sub> 0.1M at pH 7. b. H<sub>3</sub>PO<sub>4</sub> 0.1M + 1% H<sub>2</sub>O<sub>2</sub> at pH 7. Frequency: 1 kHz.

In an attempt to explain such an evolution, further experiments were made on the basis of the  $I_{Ga} = f(V)$  curve of Fig. 9.

First, a "clean" n-type GaAs electrode was held at -1.4V, i.e., on the cathodic side of the passivation peak, for more than 2h, the differential capacitance being periodically and automatically measured after a fast microcomputer monitored shift of the potential (less than 1s) to 0.0V. The measured capacitance at 0.0V remained perfectly constant and equal to that of the "clean" surface at the same voltage  $(2 \cdot 10^{-7} \text{ F} \cdot \text{cm}^{-2} \text{ [see Fig. 13]})$  in all cases. The "new" smooth and polished surface appeared to be oxide free by ellipsometric measurements, as the "clean" surfaces were.

Second, a "clean" electrode was held at -0.75V, i.e., on the other side of the passivation peak. Capacitance measurements were performed for more than 10h in the same way as before. A fast increase followed by a slow continuous decrease of the capacitance was observed. Ellipsometric measurements proved the growth of an oxide layer which appeared to be linked with the change of the electrode capacitance.

Third, Mott-Schottky plots were obtained for such a deliberately oxidized sample in the different media:  $\rm H_3PO_4$  0.1M, pH 7 and  $\rm H_3PO_4$  0.1M + 1%  $\rm H_2O_2$ , pH 7. The results showed a good linearity for both solutions over a large range of potentials. This shows that the oxide evolution rate could be neglected during these experiments. Figure 13 shows that plots obtained in both media were identical, but were shifted towards positive potentials compared with the plots obtained for the "clean" sample in the first solution. It is worth noticing that such a phenomenon in a nonaqueous medium, probably due to a large potential drop across the oxide layer, has already been reported by Morisson et al. (27), as has been the lower slope for the oxidized sample compared with the "clean" one. We have no explanation for this phenomenon (note the two scales used in Fig. 13).

All these experiments clearly confirm that in  $H_2O_2$  medium: (i) the decrease of the n-GaAs dissolution rate, above -1.1V (Fig. 9) is due to a passivation of the semiconductor caused by the growth of an oxide layer. (ii) the GaAs surface on the cathodic side of these passivation peaks can be considered oxide free.

Application: selective etching.—From a knowledge of the  $I_{Ga} = f(V)$  curves it is possible to explore a new way of selective etching of the three III-V semiconductors considered here. Referring to the previous

sections concerning the behavior of these materials at pH 7 (when the passivation is very efficient) between -1.5 and -1.1V, GaAlAs is protected against corrosion by passivation, while GaAs dissolves. The same is observed for GaAsP between -1.3 and -1.1V. If the voltage of an heterostructure involving GaAs and GaAlAs, or GaAsP, is fixed within these ranges, dissolution of GaAs alone will occur. This selective process of dissolution involves both the choice of an applied voltage and the passivation phenomenon in oxidizing media. Usually these methods are used independently of each other, the latter being carried out at rest potential etching.

Preliminary experiments have been performed on a GaAs/GaAlAs heterostructure at -1.2V in a  $\rm H_3PO_4$  0.1M + 1%  $\rm H_2O_2$  aqueous solution at pH 7. Dissolution began from the GaAs surface. The approximate observed selectivity ratio (etching rate of GaAs upon etching rate of GaAlAs) was about 10, further experiments are needed for a better determination of this ratio.

It is worth noting that afterwards GaAlAs interface exhibits a smooth, mirrorlike surface. This is probably due to the fact that at this potential (-1.2V) the remaining oxide layer is thin and helps the polishing process by a diffusion mechanism. The quality of the surface after such selective attack appears to be one of the most important advantages of the method.

The same technique was applied to GaAs/GaAsP heterostructure. In this case, the nature of the surface is satisfactory enough for practical applications but the smoothness is not as marked as for GaAlAs. Therefore, for this last type of heterostructure there is no great advantage in using the technique with applied voltage, since, as already stated, selectivity is obtained directly in acid or alkaline media at the rest potential.

The experiments described above show that a precise knowledge of electrochemical behavior permits a rapid determination of possible selective etching procedures.

# **Conclusions**

Using impedance and ellipsometric measurements, we have shown that a method based on direct analysis of corrosion products of the semiconductor under corrosion conditions leads to a better understanding of the corrosion mechanisms involved for the III-V compounds concerned in this study. The etching behavior of  $\rm H_2O_2$  appears to be controlled by an oxide

layer formation which depends to a great extent on the pH. From this result new experimental conditions may be established in order to solve practical problems concerning selective etching.

## Acknowledgments

We are pleased to acknowledge that this work was supported by the French Direction des Recherches et Etudes Militaires (DRET) under contract no. 80-34-169-00-470-75-01. We would like to thank Dr. J. Joseph and Dr. A. Gagnaire for their useful contribution (ellipsometric measurements) and D. Richartz (RTC) for his technical assistance.

Manuscript submitted June 2, 1982; revised manuscript received ca. Nov. 1, 1982.

Ecole Centrale de Lyon assisted in meeting the publication costs of this article.

#### REFERENCES

- 1. R. P. Tijburg and T. Van Dongen, This Journal,
- 123, 687 (1976).

  2. L. Hollan, J. C. Tranchant, and R. Memming, *ibid.*, 126, 855 (1979).
- 3. R. A. Logan and F. K. Reinhart, J. Appl. Phys., 44,
- C. E. Hurwitz, J. A. Rossi, J. J. Hsien, and C. M. Wolfe, Appl. Phys. Lett., 27, 241 (1975).
   J. L. Merz and R. A. Logan, J. Appl. Phys., 47, 3503 (1976).
- 6. J. L. Merz, R. A. Logan, and A. M. Sergent, IEEE J. Quantum Electron., qe-15, 72 (1979)
- 7. R. Memming, Philips Tech. Rev., 38, 160 (1978/
- "Photoeffects at Semiconductor-Electrolyte Interfaces," A. J. Nozik, Editor, A.C.S. Symp. Series No. 146, American Chemical Society, Washington, DC (1981).
   S. R. Morrison, "Electrochemistry at Semiconductor and Oxidized Metals Electrodes," Plenum Proce Nature (1992).
- Press, New York (1980).

  10. H. Gerischer, in "Physical Chemistry, an Advanced Treatise," Vol. IX-A, p. 483, H. Eyring, Editor, Academic Press (1970).

- 11. R. Memming and G. Schwandt, *Electrochim. Acta*, 13, 1299 (1968).
- 12. H. Gerischer and W. Mindt, *ibid.*, **13**, 1329 (1968). 13. H. Gerischer and W. Mindt, *Surf. Sci.*, **4**, 440
- 14. R. Memming, Ber. Bunsenges. Phys. Chem., 81, 732
- (1977).
  15. T. Inoue, T. Watanabe, A. Fujishima, and K. Honda, This Journal, 127, 719 (1977).
  T. M. J. Madou, and S. R. Morrisson,
- K. W. Frese, Jr., M. J. Madou, and S. R. Morrisson, J. Phys. Chem., 84, 3172 (1980).
- 17. B. Miller, S. Menezes, and A. Heller, J. Electroanal. Chem., 94, 85 (1978)
- 18. T. Ambridge and M. M. Faktor, J. Appl. Electrochem., 5, 319 (1975). 19. W. W. Harvey, This Journal, 114, 473 (1967).
- 20. A. Gagnaire and J. Joseph, C.R. Acad. Sci., Ser. B, 293, 357 (1981)
- 21. F. Cardon and W. P. Gomes, J. Phys. D., 11, L63
- F. El Halouani, H. Traore, G. Allais, and A. Deschanvres, Surf. Sci., 79, 498 (1979).
- 23. R. Memming, This Journal, 116, 785 (1969).
  24. R. Memming, in "Electroanalytical Chemistry,"
  A. J. Bard, Editor, Vol. 11, p. 1, M. Dekker, Inc., (1979).
- 25. H. Gerischer, N. Müller, and O. Haas, J. Electro-
- anal. Chem., 119, 41 (1981).

  26. J. C. Tranchant, L. Hollan, and R. Memming, This
- Journal, 125, 1185 (1978). 27. K. W. Frese and S. R. Morrisson, ibid., 126, 1235 (1979).
- J. M. Palau, E. Testemale, and L. Lassabatere, J. Vac. Sci. Technol., 19, 192 (1981).
- W. E. Spicer, I. Lindau, P. Skeath, and C. Y. Lu, ibid., 17, 1019 (1980).
- 30. E. Kamieniecki and G. Cooperman, ibid., 19, 453 (1981).
- A. Munoz-Yague, J. Piqueras, and N. Fabre, This Journal, 128, 149 (1981).
   H. Gerischer, D. M. Kolb, and J. K. Sass, Adv. Phys., 27, 437 (1978).
   D. W. Shew, This Learner, 127, 274 (1991).
- 33. D. W. Shaw, This Journal, 127, 874 (1981).
  34. M. Pourbaix, "Atlas d'Equilibres Electrochimiques," Gauthier-Villars et Cie, Editor, Paris (1963).

# Catalytic Activity of Iron, Nickel, and Nickel-Phosphorus in **Electroless Nickel Plating**

J. Flis<sup>1</sup> and D. J. Duquette

Department of Materials Engineering, Rensselaer Polytechnic Institute, Troy, New York 12181

# ABSTRACT

The catalytic activity for electrooxidation of hypophosphite and electroless nickel plating on iron, nickel, and electrolessly plated nickel (with 2.2-2.9 weight percent (w/o) P) was investigated in an ammoniacal solution of pH 8.8 at 50°C by potential measurements and linear sweep voltammetry from -0.3V to 0.92V vs. SCE. Cathodic polarization of any of the substrates (in 0.1M H<sub>2</sub>SO<sub>4</sub>) before testing or permeation of hydrogen through iron foils during testing reduced the incubation time for electroless plating, increased anodic dissolution of the substrates in the passive region, and increased the hypophosphite electrooxidation on nickel and nickel-phosphorus at potentials of thermodynamic stability for nickel oxides or hydroxides. The nickel-phosphorus substrate exhibited significantly higher activity than pure nickel, in a similar manner to the effect of cathodic polarization. The effect of cathodic polarization and hydrogen is associated with the electrochemical reduction of surface oxides, whereas the higher activity of nickel-phosphorus deposits (as compared to that of pure nickel) is explained by the lower protectivity of surface oxides on these deposits.

Electroless nickel plating from hypophosphite solutions proceeds spontaneously on many metal surfaces (1-5), although the specifics of this process may be of a different nature. Some noble metals (palladium,

from Institute of Physical Chemistry, 01-224 Warszawa, Poland.

Key words: electroless, nickel plating, iron, nickel, nickel-phosphorus.

rhodium, nickel, cobalt, gold) possess an intrinsic catalytic ability to induce electrooxidation of hypophosphite, and electroless nickel plating; whereas some active metals become catalytic due to the deposition of nickel from a solution by a displacement reaction. The latter phenomenon has been shown for iron, aluminum. and beryllium (2), gallium and thallium (6), magnesium, zinc, and manganese. The